ARL-TR-7542 ● DEC 2015

US Army Research Laboratory

Optimization of Strontium Titanate ($SrTiO_3$) Thin Films Fabricated by Metal Organic Chemical Vapor Deposition (MOCVD) for Microwave-Tunable Devices

by Erik Enriquez, D Shreiber, SG Hirsch, C Hubbard, E Ngo, and MW Cole

NOTICES

Disclaimers

The findings in this report are not to be construed as an official Department of the Army position unless so designated by other authorized documents.

Citation of manufacturer's or trade names does not constitute an official endorsement or approval of the use thereof.

Destroy this report when it is no longer needed. Do not return it to the originator.

ARL-TR-7542 ● DEC 2015

US Army Research Laboratory

Optimization of Strontium Titanate ($SrTiO_3$) Thin Films Fabricated by Metal Organic Chemical Vapor Deposition (MOCVD) for Microwave-Tunable Devices

by Erik Enriquez
University of Texas San Antonio

D Shreiber
Oak Ridge Institute for Science and Education

SG Hirsch, C Hubbard, E Ngo, and MW Cole
Weapons and Materials Research Directorate, ARL

REPORT DOCUMENTATION PAGE

Form Approved
OMB No. 0704-0188

1. REPORT DATE (DD-MM-YYYY)	2. REPORT TYPE	3. DATES COVERED (From - To)
December 2015	Final	May 2014–October 2014

4. TITLE AND SUBTITLE
Optimization of Strontium Titanate ($SrTiO_3$) Thin Films Fabricated by Metal Organic Chemical Vapor Deposition (MOCVD) for Microwave-Tunable Devices

5a. CONTRACT NUMBER

5b. GRANT NUMBER

5c. PROGRAM ELEMENT NUMBER

6. AUTHOR(S)
Erik Enriquez, D Shreiber, SG Hirsch, C Hubbard, E Ngo, and MW Cole

5d. PROJECT NUMBER

5e. TASK NUMBER

5f. WORK UNIT NUMBER

7. PERFORMING ORGANIZATION NAME(S) AND ADDRESS(ES)
US Army Research Laboratory
ATTN: RDRL-WMM-E
Aberdeen Proving Ground, MD 21005-5069

8. PERFORMING ORGANIZATION REPORT NUMBER
ARL-TR-7542

9. SPONSORING/MONITORING AGENCY NAME(S) AND ADDRESS(ES)

10. SPONSOR/MONITOR'S ACRONYM(S)

11. SPONSOR/MONITOR'S REPORT NUMBER(S)

12. DISTRIBUTION/AVAILABILITY STATEMENT
Approved for public release; distribution is unlimited.

13. SUPPLEMENTARY NOTES

14. ABSTRACT
An introductory overview of commonly employed deposition methods for strontium titanate (STO) thin films with previously achieved dielectric properties is presented. For the US Army Research Laboratory's Gen 2 complex oxide metal organic chemical vapor deposition (MOCVD) system, STO thin films were grown on a platinized silicon substrate, $Pt/TiO_2/SiO_2/Si$, or PtSi. All STO films were characterized by X-ray diffraction, scanning electron microscopy, atomic force microscopy, and energy dispersive spectroscopy. Studies of mass flow rates and total gas flow rates were performed to investigate their respective roles in the resulting STO film characteristics. Our work demonstrated a significant increase in the quality of the optimized STO thin films with respect to STO films grown prior to the MOCVD hardware and growth parameter modifications. Optimized STO films had a tunability of 20%, a dielectric constant of 200, and loss tangent of less than 1% at 100 kHz.

15. SUBJECT TERMS
strontium titanate, STO, thin films, MOCVD, growth and processing

16. SECURITY CLASSIFICATION OF:			17. LIMITATION OF ABSTRACT	18. NUMBER OF PAGES	19a. NAME OF RESPONSIBLE PERSON
a. REPORT	b. ABSTRACT	c. THIS PAGE			MW Cole
Unclassified	Unclassified	Unclassified	UU	40	19b. TELEPHONE NUMBER (Include area code) 410-306-0747

Contents

List of Figures

List of Tables

Acknowledgments

The lead author of this manuscript, Erik Enriquez, would like to thank the US Army Research Laboratory and the dedicated individuals of the Integrated Electromagnetic Materials Research Team for making this research possible. I would especially like to thank MW Cole for her mentorship, inspiration, continual help, and for her fruitful and thoughtful contributions that enabled this research.

INTENTIONALLY LEFT BLANK.

1. Introduction and Background

1.1 Strontium Titanate (STO) in Microwave-Tunable Devices

STO is an incipient ferroelectric material with physical and electrical properties that make it a promising candidate for a broad range of technology applications, notably those that require frequency- and phase-agile electronic components such as varactors, voltage-controlled oscillators, and phased-array antennas. For device applications, STO thin films are particularly attractive due to their high dielectric constant (~300), low loss tangent or dissipation factor in the radio frequency (RF) range ($D = \tan\delta = \varepsilon''/\varepsilon'$), and because they exhibit a tunability of their dielectric constant across a broad operational frequency range. The tunability of STO is a measure of the change in dielectric constant that occurs in the media with the application of an external bias voltage.

$$Tunability = \frac{\varepsilon_r(0) - \varepsilon_r(V)}{\varepsilon_r(0)} \times 100\%, \quad (1)$$

where $\varepsilon_r(0)$ represents the relative dielectric constant of the material without applied voltage and $\varepsilon_r(V)$ is the relative dielectric constant with an applied external voltage, V. In addition to the desirable intrinsic properties of STO, the use of thin films requires less material and significantly reduced power consumption, so the cost benefit of STO thin films allows for the potential of phase- and frequency-agile electronics in much smaller form factors with much broader potential applications.[1]

Although working with thin film STO has many inherent and potential advantages, there are several persistent challenges that researchers have directed efforts to overcoming in order to adapt these materials to device applications. Dielectric loss, which acts as a dampening of an inserted RF signal, is a crucial issue, and a substantial amount of the recent research in STO thin films has dealt with minimizing this value. The value is usually less than 1,0 and thus often is referred to as a percentage. For tunable device applications, the RF loss of these dielectric thin films typically must be below a few percent. The external sources of loss, such as conductor interface losses and various losses that inevitably arise from device design, must be considered when these films are incorporated into device structures, so minimizing losses from the dielectric material is a crucial element of optimization and device realization. Leakage current, which results from the imperfect insulating properties of any dielectric material, must also be minimized to reduce the power draw of device components.

While there are various techniques employed by researchers to decrease dielectric loss in STO, optimization is difficult due to the sensitivity of STO to processing conditions. Although the dielectric properties of STO have been shown to improve with film quality (highly textured films, smooth interfaces with minimal defects, and homogeneity), growth temperatures, growth techniques, substrate material, and postprocessing treatments can all affect the resulting properties of STO thin films. An excellent review of the device requirements for dielectric thin films is discussed by Dey and Alluri.[2] Each device application has its own set of performance requirements, but even if these requirements can be achieved through high-quality thin film deposition, the technique used in production must also be suitable for scaling to production levels with reasonable cost and throughput as well as a high degree of uniformity across batches and deposition systems.

1.2 Reports of STO Performance

There are various STO deposition techniques, and within each technique there are many variations in preparation, equipment, and procedures. Even measurements of physical and electrical properties carry advantages, limitations, and biases unique to each experimental setup. This variety in techniques and characterization can provide many insights into the complex growth mechanisms of STO, but it also serves as a source of ambiguity in parallel research efforts to understand and optimize the physical and electrical properties of STO. Deposition techniques can be classified as either physical or chemical processes, although there is a range of methods that employ both simultaneously. Several reviews highlight the advantages and limitations of each deposition technique for complex oxide thin films such as STO, namely the detailed introduction and discussions by Ohring,[3] Kern and Schuegraf,[4] and an excellent review by Subramanyam et al.[5] Although other promising techniques such as reactive co-evaporation have been pursued in the deposition of STO,[6–8] the following sections will focus on widely established STO deposition techniques. A brief overview of the main deposition techniques is presented in Table 1.

Table 1 Overview of general advantages and limitations of major growth techniques used in STO fabrication[3–5]

Growth technique	Advantages	Limitations
Pulsed laser deposition (PLD)	• High growth rates • Excellent compositional control • Highly epitaxial thin films	• Rough surfaces can result from macroscopic target particles impinging on surface • High cost • Low throughput • Very limited area of uniform deposition (~1 inch squared)
RF sputtering	• Large-area deposition • Industry standard technique • Cost-effective	• Difficult to control film stoichiometry • Low growth rates • Low efficiency usage of target materials
Chemical solution deposition (CSD)	• Low equipment cost • High uniformity • Industry standard technique • Precise control of stoichiometry and thickness	• Complexity/compatibility of precursors for multicomponent oxide films • Ligand decomposition reactions can lead to cracks and porous film structures
Molecular beam epitaxy (MBE)	• Very high quality • Low density of formed defect sites • Low–moderate processing temperatures • Very high degree of control of film structure and growth modes	• Low deposition rates • Very high equipment and production cost • Strict maintenance requirements • Narrow window of processing parameters to obtain stoichiometric oxide thin films
Chemical vapor deposition (CVD)	• High throughput • Potential for high structural quality and film epitaxy • Excellent control of film stoichiometry and thickness • Large area uniformity and potential for complex structure coating	• Optimized system design and maintenance are crucial to efficiency and quality of thin films • Many techniques for precision delivery of precursors significantly increase equipment cost and complexity, and require elaborate calibration

1.2.1 Pulsed Laser Deposition (PLD)

PLD, also known as laser ablation, is a physical deposition technique in which dense solid-state target materials are flash evaporated by an incident laser radiation source. It is carried out in a low-pressure environment and is the most popular thin film deposition technique in laboratory and academic research settings due to the exceptional quality of thin films it can produce with fewer process variables than those required by RF sputtering and chemical deposition techniques. Because of the nature of evaporation and low-pressure deposition environment, the composition of STO and other complex oxide thin films fabricated by PLD can be controlled very precisely and without the need for extensive process optimization by selection of the target material.[9,10] Also, since PLD employs purely physical deposition mechanisms, there are no organics or reaction byproducts inherently present in the process that can contaminate the thin film. This high degree of control has allowed researchers with the means to fabricate high-quality, highly epitaxial and pure STO thin films, which has aided greatly in the fundamental studies of the role of substrate,[11] strain,[12–18] composition,[19,20] and film thickness[21] on the dielectric properties of STO on various substrate materials. An overview of experimental values for STO thin films fabricated by PLD is presented in Table 2.

Table 2 Selection of available dielectric property data of STO thin films produced by PLD. Relative permittivity, ε, dielectric loss, tanδ, and tunability data for all sources were collected at room temperature, 100 kHz.

Reference	Substrate	Processing temperature (°C)	Thickness (nm)	ε	tanδ	Tunability	Leakage current (A/cm^2)
Tachiki et al.[22]	LSMO/MgO	600	86	320	NR	56%	NR
Iwabuchi et al.[23]	YBCO/MgO	660	64	120	0.07	27%	NR
Roy et al.[24]	PtSi	500	500	240	0.02	6%	10^{-5}
Rao and Krupanidihi[25]	PtSi	600	1,000	225	0.03	2%	10^{-5}
Boikov and Claeson[26]	SRO/LAO	780	800	400	0.01	NR	NR
Breckenfeld et al.[20]	Nb:STO	750	200	275	0.01	NR	NR

Note: NR = not reported; LSMO = lanthanum strontium manganite; MgO = magnesium oxide; Pt = platinum; YBCO = yttrium barium copper oxide; LAO = lanthium aluminate.

While PLD has provided many valuable insights on the relationship of physical properties, dielectric phenomena, and device performance, its major limitations are prohibitive cost and small sample area. Thin films fabricated by PLD are typically limited to about a 1-inch-squared uniform deposition area. While some emerging technology holds significant promise for the expansion of PLD techniques to include uniform deposition of 4- to 8-inch wafers for industry applications, currently it remains mainly a laboratory-scale fabrication technique.[5]

PLD also requires a high equipment investment for the laser source and optics in addition to the vacuum equipment. To bridge the gap between the fundamental research and potential of STO thin films uncovered by PLD fabrication and device application, optimization by lower-cost techniques such as CSD and metal organic chemical vapor deposition (MOCVD) techniques are required.

1.2.2 Radio Frequency Sputtering

RF sputtering is another highly favored thin film deposition method for STO. Sputter deposition relies on large electric field potentials to strike target surfaces with ionized gas atoms, either inert or reactive. Impinging gas atoms with high kinetic energy release particles from the target surface into the vapor phase, which then rain down on a substrate material to generate a thin film. This technique is desirable for its high throughput thanks to its potential for large area deposition, which PLD lacks.[4,27] Sputter systems range from small laboratory setups to industrial production models that handle batches of wafers simultaneously. Similar to PLD, sputtering has shown potential to produce very-high-quality thin films with superb microstructural and electrical properties.[28–32]

Thin films fabricated by sputter techniques, although widely used for the deposition of STO, are extremely sensitive to processing conditions. Compositional control is often very challenging in multicomponent oxide thin films due to the differences in yield and sticking coefficients in various elements. Even for a target of a fixed composition, parameters such as substrate-target distance, angle of target, power, and ambient environment have all been shown to affect the resulting composition, microstructure, and homogeneity of the resulting thin film.[33–37] This makes optimization and reproducibility across even similar systems very difficult. For this reason, RF sputtering has met many challenges in producing smooth, uniform thin films over large surface areas compared with techniques such as MBE, CSD, and MOCVD. Experimental values from several available literature sources for STO thin films obtained by sputter deposition techniques are presented in Table 3.

Table 3 Selection of available dielectric property data of STO thin films produced by sputter deposition techniques. Unless otherwise noted, relative permittivity, ε, dielectric loss, tanδ, and tunability data for all sources were collected at room temperature and 100 kHz.

Reference	Substrate	Processing temperature (°C)	Thickness (nm)	ε	tanδ	Tunability	Leakage current (A/cm^2)
Boesch et al.[28]	Pt/STO	700	160	354	0.001	NR	NR
Abe et al.[38]	Pt/MgO	400	92	280	NR	64%	10^{-7}
Komatsu et al.[35]	Pt/MgO	600	50	450	NR	75%	10^{-8}
Itsumi et al.[39]	PtSi	400	100	200	NR	NR	10^{-9}
Pennebak[40]	Au/Al_2O_3	500	240	220	0.02	54%	10^{-4}
Peng et al.[41]	PtSi	700	1,200	219	0.1	2%	10^{-6}
Lu et al.[42]	Pt/Al_2O_3	700	100	280[a]	0.0017[a]	32%[a]	10^{-8}

[a] Measurement data was recorded at 1 MHz; Au = gold; NR = no result.

1.2.3 Molecular Beam Epitaxy

MBE is a method of deposition similar to thermal and ablation evaporation techniques such as PLD and is one of the most precise techniques in thin film deposition available. MBE deposition is conducted in an ultrahigh-vacuum environment (~10^{-10} Torr) and often uses effusion cells, electron beams, or laser sources to flash evaporate target materials. Due to the ultrahigh-vacuum environment, the evaporated molecules have a much longer mean free path than the distance from the evaporation cell to the substrate, which results in a low probability of vapor phase collisions during transport. Thus, a target material evaporated through a small opening travels as a molecular "beam" with a small angle spread generated at the evaporation cell aperture. When the deposition rate is low enough, such that the time needed to generate a monolayer is greater than the surface-diffusion-incorporation time (τ_{di}), high-quality thin films can be produced with monolayer deposition control.[43,44] The precise control of evaporation and deposition in MBE has produced many great in situ studies and characterization of structure-property relationships in STO thin films.[45–51] Since physical MBE processes do not depend on chemical reactions when target materials are converted to solid-state from the vapor phase, lower processing temperatures can be employed without the issue of contaminants and remaining byproducts that other high-quality chemical deposition techniques such as CSD, atomic layer deposition (ALD), and MOCVD have commonly faced.[52,53]

Although MBE processes have been shown to provide very-high-quality thin films in semiconductor materials, the growth of oxide materials provides great challenges for MBE. Oxide thin films grown in such low-pressure environments have suffered from oxygen nonstoichiometry and compositional difficulties with the simultaneous deposition of multicomponent oxides. Jalan et al.[54] have reported on focused efforts to establish the narrow growth window of processing

conditions in which stoichiometric STO can be achieved without the formation of undesirable strontium oxide (SrO) or titanium dioxide (TiO_2) phases. In addition to concerns of stoichiometry control, MBE carries a prohibitively high equipment and operational cost for scalable production of high-quality STO thin films. The ultrahigh vacuum conditions require specialized equipment and fitting compatibility, which carries a much higher equipment cost than high-vacuum systems traditionally used in PLD, sputtering, and CVD techniques. Maintenance for ultrahigh vacuum systems must also be strictly upheld, and even a small degree of equipment contamination, degradation, or misuse can lead to significant downtime and costly repairs to reclaim the ultrahigh vacuum environment. The high cost, low deposition rates, and low throughput of oxide materials produced by MBE, much like PLD, has kept MBE mostly as a superb laboratory-scale fabrication technique for fundamental studies of STO physical-electrical phenomena and structure-property relationships. Experimental values from several available literature sources for STO thin films obtained by sputter deposition techniques are presented in Table 4.

Table 4 Selection of available dielectric property data of STO thin films produced by MBE. Relative permittivity, ε, dielectric loss, tanδ, and tunability data for all sources were collected at room temperature.

Reference	Substrate	Processing temperature (°C)	Thickness (nm)	ε	tanδ	Tunability	Leakage current (A/cm^2)
Wu et al.[53]	GaAs	650	300	240 (100 kHz)	0.018 (100 kHz)	NR	NR
Nakamura et al.[52]	YBCO/STO	480	175	300 (100 kHz)	NR	NR	10^{-8}
Wu et al.[50]	YBCO/LAO	800	300	250 (10 kHz)	0.011 (10 kHz)	NR	NR
Hao et al.[48]	SRO/STO	760	NR	294 (1 kHz)	0.004 (1 kHz)	NR	NR

Notes: GaAs = gallium arsenide.

1.2.4 Chemical Solution Deposition

CSD is a broad term to classify deposition techniques that generally employ liquid-state precursor materials to generate a solid-state thin film. STO thin film growth by CSD techniques include many variations and monikers, such as metalorganic solution deposition (MOSD)[55,56] or metalorganic decomposition,[57] sol-gel deposition,[58–60] polymeric precursor deposition,[61–63] and liquid-phase deposition.[64] CSD techniques for STO mainly employ spin-coating or immersion of precursor materials onto a substrate surface, followed by pyrolysis, which removes solution, gel and/or ligand chemicals to produce a solid-state STO film. At low temperatures, these films have been shown to be mostly amorphous, and can be annealed at higher temperatures to ensure further removal of contaminants and meta-stable phases and to crystallize the thin films.

CSD techniques excel in their potential to control stoichiometry of thin films, which can be seen in research modifying the composition and nonstoichiometry of STO.[65–67] CSD techniques have also produced uniform STO thin films with very smooth surfaces, usually to within 1–3 nm of root-mean-square roughness values on high-quality substrates, with the potential to uniformly coat larger area substrates than those obtainable by PLD and RF sputtering methods.[56,60,62,63,68] In addition, CSD techniques are industry standard and require notably lower equipment and operation costs than vacuum deposition techniques. Although CSD techniques are cost-effective, multicomponent oxide materials such as STO require complex chemical reactions while maintaining compatibility between multiple precursors as well as appropriate viscosity and ambient sensitivity to produce uniform and high-purity thin films. STO thin films grown by CSD techniques typically produce amorphous-to-polycrystalline thin films, dependent on processing conditions, but several reports note that micro-cracks or porous structures in topography are challenges in STO optimization.[56,58,60,68–70] Notable overviews of STO films produced by CSD techniques have been detailed by Weiss et al.,[56] as well as select comparisons to other deposition techniques by Pontes et al.[62] Select experimental values for STO thin films obtained by CSD methods are presented in Table 5.

Table 5 Selection of available dielectric property data of STO thin films produced by CSD methods. Relative permittivity, ε, dielectric loss, tanδ, and tunability data for all sources were collected at room temperature, 100 kHz.

Reference (technique)	Substrate	Processing temperature (°C, pyrolysis/anneal)	Thickness (nm)	ε	tanδ	Tunability	Leakage current (A/cm^2)
Weiss et al.[56] (MOSD)	PtSi	400/750	147	331	0.021	28%	10^{-6}
Dawley et al.[71] (CSD)	Nickel tape	300/900	800	250	0.003	29%	NR
Pontes et al.[62] (polymeric)	PtSi	400/700	600	475	0.05	8%	NR
Pontes et al.[63] (Polymeric)	PtSi	400/600	360	250	0.01	5%	10^{-7}
Tsuzuki et al.[60] (sol-gel)	PtSi	120/700	180	170	0.01–0.02	NR	NR
Thomas et al.[59] (sol-gel)	Stainless steel	350/650	1,100	150	0.35	2%	NR
Kamalasanan et al.[58] (sol-gel)	Stainless steel	500/700	600	131	0.022	3%	10^{-7}

1.2.5 Chemical Vapor Deposition

CVD techniques present a unique opportunity in the fabrication of complex oxide thin films. The umbrella of CVD includes many techniques and modifications, such as MOCVD, plasma-enhanced atmospheric-pressure laser CVD, and ALD, among others. Various mechanisms can be employed for CVD, but mostly they involve a target species incorporated into a ligand structure that allows for conversion into vapor phase. Upon transport to a substrate, chemical reactions by pyrolysis or other means strip the ligand from the target species and allow for diffusion and nucleation on the substrate surface. Although there are many variations of CVD methods, overall it has shown the potential for the high degree of uniformity over large deposition areas sought out in other industrial techniques such as sputter deposition and CSD, but has also shown a high degree of structural, compositional, and thickness control without the use of the ultrahigh-vacuum environments of MBE or the limitations of PLD techniques. Although MBE and PLD are still largely unmatched in their respective advantages, CVD brings a scalable precision technique in the deposition of complex oxide thin films. For this reason, CVD has attracted much attention for fundamental as well as industrial applications.[72–75]

MOCVD further improves upon this technique by incorporating metalorganic precursors, many of which are less toxic, more stable, and can be easily converted to vapor phase at notably lower temperatures than their traditional CVD counterparts.[75] The lower evaporation and processing temperatures provide lower operational costs and equipment restrictions than other precision deposition techniques. Although MOCVD research has reported various high-quality thin film achievements, the variations in reactor and precursor deliver technology are staggering, all of which play a significant role in the optimization conditions of complex oxide thin film production.[76] Because of this, reactor design and precursor supply for the development of MOCVD systems depend heavily on flow modeling and optimization efforts.[77–81]

Another challenge is that precursor delivery control methods such as liquid injection and aerosol delivery require elaborate calibration and high-cost precision equipment. The US Army Research Laboratory's (ARL's) Gen 2 MOCVD system circumvents this with its unique in situ ultraviolet (UV) spectroscopy monitor, which grants precision control of precursor flow while still allowing for conventional bubbler sublimation delivery of precursor materials and is a more-cost-effective and less-complex system design. Despite the associated challenges, MOCVD remains a promising technique for the development of frequency- and phase-agile device components such as STO. A selection of some of the achievements in STO thin film production by MOCVD are presented in Table 6.

Table 6 Selection of available dielectric property data of STO thin films produced by CVD techniques. Unless otherwise noted, relative permittivity, ε, dielectric loss, tanδ, and tunability data for all sources were collected at room temperature, 100 kHz.

Reference (technique)	Substrate	Processing temperature (°C)	Thickness (nm)	ε	tanδ	Tunability	Leakage current (A/cm^2)
Funakubo et al.[82] (CVD)	Pt/MgO	800	600	220	0.01	NR	NR
Liang et al.[83] (PEMOCVD)	YBCO/LAO	750	150	315	NR	5%	10^{-6}
Yamaguchi et al.[84] (MOCVD)	Pt/TaO_x/Si	600	100	210	0.01	NR	10^{-7}
Cho et al.[85] (MOCVD)	Pt/SiO_2/Si	550	50	150	NR	NR	10^{-7}
Grill et al.[86] (MOCVD)	PtSi	700	320	131	0.02	NR	10^{-7}
Kang et al.[87] (MOCVD)	PtSi	650	30	220 (10 kHz)	0.0025 (10 kHz)	16% (10 kHz)	10^{-7}
Lee et al.[88] (ALD)	Ru/Ta_2O_5/ SiO_2/Si	700	20	108	0.07	11%	10^{-7}

Note: PEMOCVD = plasma-enhanced metalorganic chemical vapor deposition.

2. STO Optimization Studies for ARL's MOCVD System

ARL's MOCVD system, developed as a technology transfer collaboration with the California Institute of Technology and referred to here as the Gen 2 system, is currently in development. Recently, stoichiometric STO thin films were achieved using this system for the first time with the aid of hardware and process modifications to protect the sample from precursor contaminants. Although the interface and film quality was notably improved, inhomogeneity across the substrate surface persisted, particularly at the sample edges. Optical and SEM cross-sectional comparisons of STO films fabricated before and after hardware modifications are presented in Fig. 1. After observation of the persistent edge effects on as-deposited STO films that were grown after modifying the hardware, the attention of the researchers was directed to investigating the growth conditions that might be governing the observed phenomenon and to reduce the film inhomogeneity as much as possible.

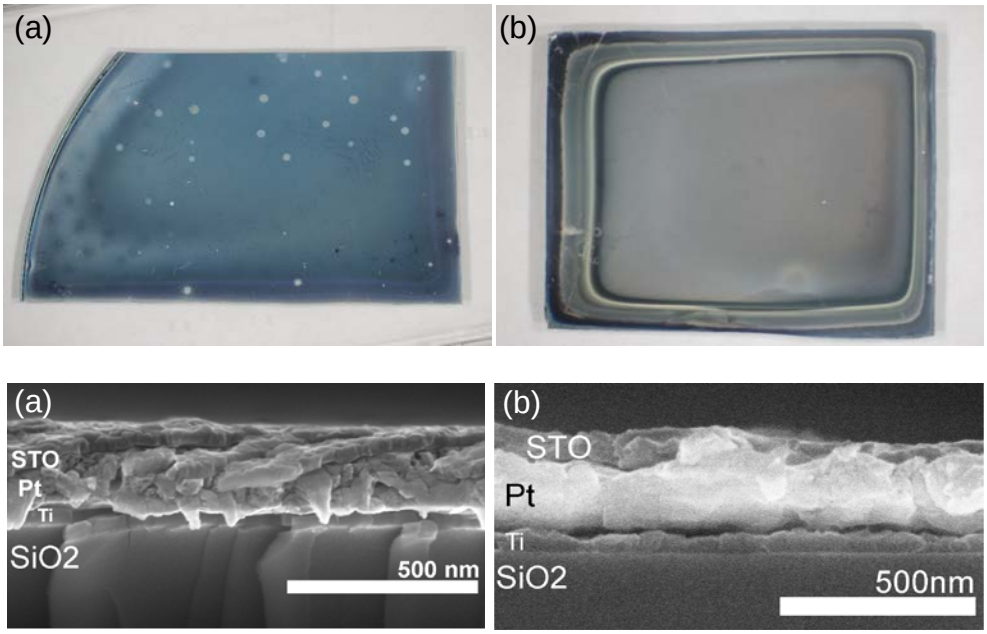

Fig. 1 Film surface (top) and scanning electron microscopy (SEM) cross-sectional images (bottom) of STO films fabricated by ARL's Gen 2 MOCVD system a) before and b) after hardware and process modifications were made. Visual inhomogeneity in 1b was confirmed to be of varying thickness.

2.1 Carrier Gas Flow Optimization

Prior to the modification of hardware components to the Gen 2 system, it was proposed that in the presence of the large number of variables involved in film deposition by MOCVD technique it was possible that deposition conditions were contributing to the inhomogeneity of film thickness over the sample surface. In developing the original Gen 1 system at the California Institute of Technology, a great deal of effort was dedicated to modeling the required flow and deposition process that would allow for laminar gas flow and produce uniform deposition across the sample. However, design changes in the Gen 2 system (in particular the size of the showerhead and the structure of the sample heating element) could have impacted the deposition process significantly.[77,89,90] With an ambiguity in the effects of total flow on the uniformity of as-deposited films, empirical investigations were conducted to study the effects of total gas flow rates on resulting film uniformity. The flow of argon (Ar) gas is used to carry a flow of precursor species through the bubblers and into the growth chamber, as well as additional gas flow that is added to keep a constant total gas flow. As-deposited samples were grown using total Ar gas flow rates of 6,000 to approximately 3,700 standard cubic centimeters per minute (sccm) and compared for compositional and microstructural homogeneity using cross-sectional optical microscopy, scanning electron microscopy (SEM), and atomic force microscopy (AFM).

2.2 Deposition Conditions

STO thin films deposited during carrier gas flow and flow rate studies are compared to optimize the process conditions with respect to the quality of thin films produced by the Gen 2 system. Deposition of the STO thin films on commercially available platinized silicon substrates, Pt(150 nm)/Ti(50 nm)/SiO_2/Si (abbreviated as PtSi), were conducted with a susceptor temperature of 620 °C and reactor pressure of 15 Torr for 60–120 min. The walls and precursor gas supply lines were maintained near 250 °C to prevent condensates. Solid-state β–Diketonate complex precursors Bis(2,2,6,6-tetramethyl-3,5-heptanedionato), purchased from Strem, and Titanium(IV) diisopropoxidebis(2,2,6,6-tetramethyl-3,5-heptanedionate), purchased from Sigma-Alrich, were used in all depositions. The Sr precursor temperature for sublimation was approximately 275 °C while the Ti precursor sublimation temperature setting was 105 °C. Individual precursor mass flow was controlled by the in situ UV spectrometer feedback loop system. A constant precursor mass flow of 15, 32, 40, 60 and 80 μmoles/min was used for depositions, with a mole ratio of 95% Sr/5% Ti and Ar carrier gas flow rates ranging from 3,700–6,000

sccm, and is discussed in the following sections. A shroud flow to promote laminar flow and prevent recirculation of 5,000 sccm was used, along with a supplemented oxygen (O_2) flow of 1,000 sccm to mitigate O_2 vacancies and nonstoichiometry. Prior to sample loading and deposition, the reactor and precursor supply lines were baked at 250 °C for at least 4 h with a total Ar carrier gas flow of 5,000 sccm to remove precursor condensates from the gas lines and showerhead.

3. Carrier Gas Flow Optimization Results

For optimization of laminar gas flow through the reactor, 2 factors must be investigated, total mass flow of precursor species and total gas flow through the showerhead. The total mass flow does not directly correlate to the precursor gas flow because the performance of any given load of precursors can decrease with each successive deposition. For the research conducted in this report, both Sr and Ti precursors were reloaded after 2 depositions, but it has been noted by the researchers that the precursors could be further depleted in between loads to maximize cost efficiency. In particular, the Ti precursor showed only a small decrease in performance, and it was extrapolated that it might be used in 4–5 depositions before reloading. With each successive deposition using a given load of precursors, a higher carrier gas flow rate of Ar is needed through the bubbler to achieve the same mass flow rate due to the decrease in yield from the used precursor material.

Samples that were deposited at a constant rate of 6,000 sccm had prominent inhomogeneous thickness edge effects, as can be seen in Fig. 1b. When the total gas flow was decreased in samples grown with a total gas flow in the range of 3,700–5,100 sccm, the observed edge effects were greatly reduced, as can be seen in Fig. 2. This effect suggests closer approximation to the laminar flow at lower gas flow rates, which results in a more uniform deposition of the thin film.

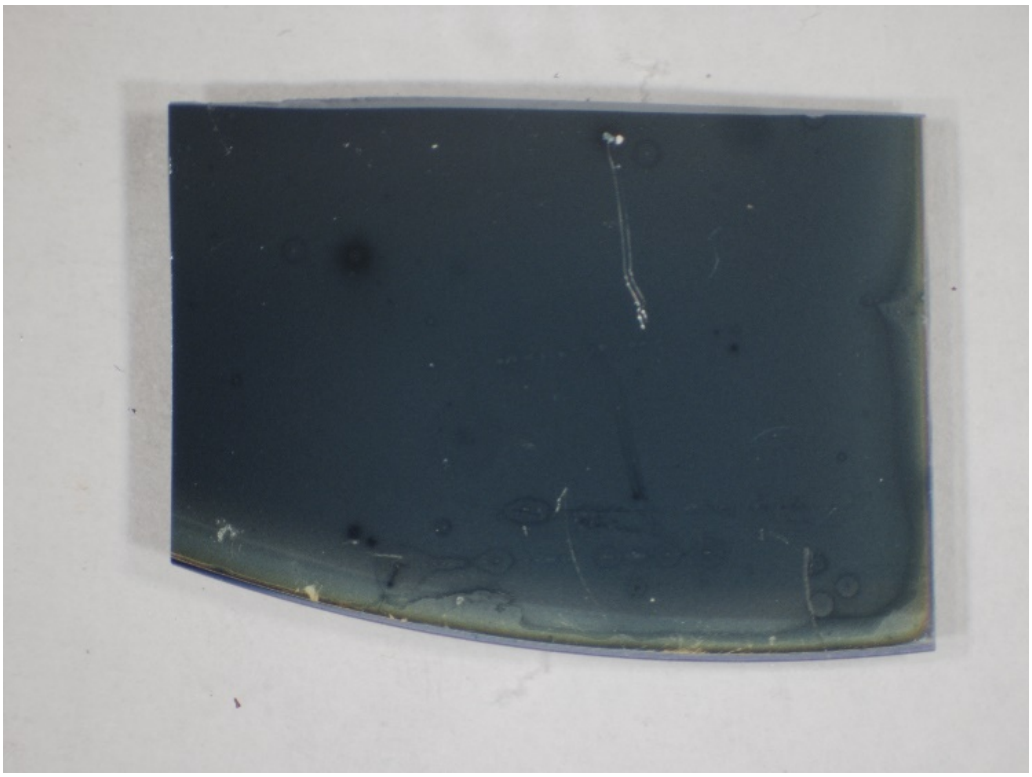

Fig. 2 Example surface of an as-deposited STO film grown on PtSi substrate at a flow rate of 3,700 sccm

4. STO Deposition Rate Study

STO films were grown on PtSi substrates at various mass flow and total gas flow rates to study the resulting film growth rates. Films were grown at mass flow rates of 15, 32, 40, 60, and 80 μmole/min at 620 °C and a 15-Torr pressure. The resulting film thicknesses were measured by cross-sectional SEM, and these data were used to determine the deposition rates with respect to the various precursor mass flow rates employed. Characterization by AFM, X-ray diffraction (XRD), and energy dispersive spectroscopy (EDS) was also performed to gain information on the film surface, composition, and structural quality of as-deposited $SrTiO_3$ samples.

The thicknesses of as-deposited STO thin films grown on PtSi substrates were compared using data from cross-sectional SEM micrographs. The calculated growth rates are shown in Fig. 3.

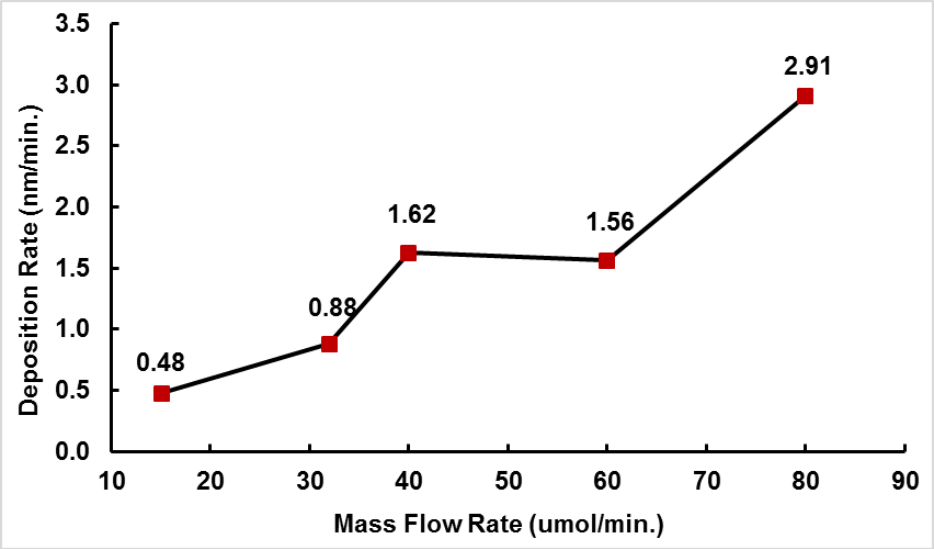

Fig. 3 Calculated growth rates of STO thin films grown on PtSi substrates at various precursor mass flow rates

The data presented in Fig. 3 combine experimental results obtained for various gas flow rates. It indicates that the deposition rate in the process is a result of a combination of factors such as the total mass flow rate and total gas flow rate. The significantly higher deposition rate at a total mass flow rate of 80 μmole/min is a result of both a higher total mass flow rate and a much lower total gas flow rate.

5. Results and Discussion

5.1 X-ray Diffraction

Glancing-angle XRD measurements were performed on all as-deposited STO thin films as well as the PtSi wafer. The data are collected in Fig. 4.

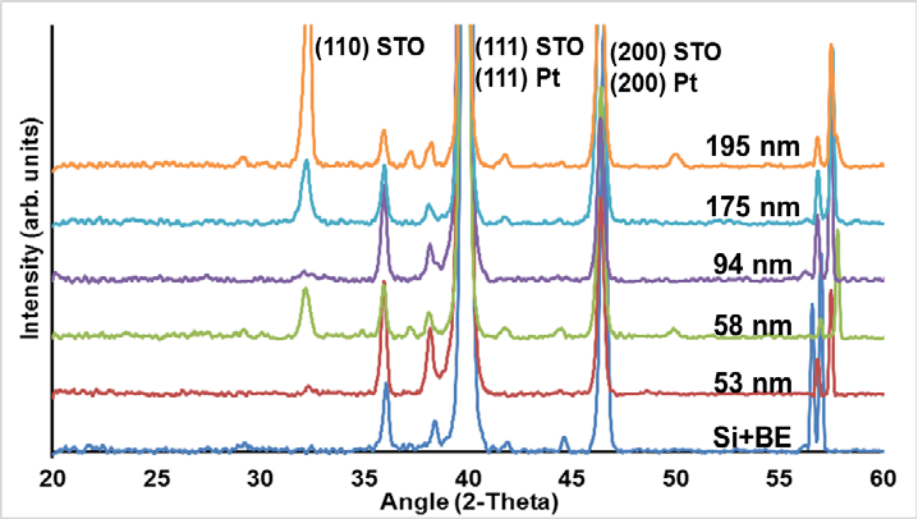

Fig. 4 Glancing-angle XRD data for as-deposited STO thin films. It is expected that the (111) and (200) STO peaks are overlapping with the respective (111) and (200) Pt peaks. Si+BE is an abbreviation for PtSi. Omega = 0.75°.

The 2-Theta scan data suggest that there is a notable (110) peak for STO. Although it cannot be confirmed by these data, it is expected that the (111) and (200) STO peaks overlap with the respective (111) and (200) peaks from the platinum in the bottom electrode. Further studies will be performed on various substrates to confirm. No secondary phases were observed, suggesting that the stoichiometric accuracy of the as-deposited STO thin films. EDS measurements were also performed for confirmation of the film stoichiometry.

5.2 Energy Dispersive Spectroscopy

EDS measurements were conducted on cross sections of all as-deposited thin films. The results demonstrated that the ratio of Sr to Ti was much nearer to the desired 1:1 ratio of $SrTiO_3$ than films grown on PtSi prior to the hardware modification and process optimization. A selected sample prior to the research conducted in this report was selected for EDS measurement and an atomic ratio for Sr:Ti of 1.92:1 was observed. Since the adhesion layer of Ti is present in the bottom electrode of the sample, the deviation from the optimal ratio of Sr:Ti is expected to be larger than what was measured, which suggests that the as-deposited film was not stoichiometric $SrTiO_3$. Measurements of chemical compositions on samples grown after the aforementioned modifications contained an average Sr:Ti ratio of 0.7:1. Given the presence of Ti in the bottom electrode (BE), this result suggests a ratio that is notably nearer to the desired 1:1 ratio than previously grown samples.

5.3 Structural and Surface Characterization

To determine the film quality in relation to the deposition growth rate, 3 as-deposited STO thin films were selected for structural and surface quality measurements by cross-sectional SEM and AFM, respectively. Selected samples were deposited at growth rates of 0.48, 1.56, and 2.91 nm/min. The data are presented in Fig. 5.

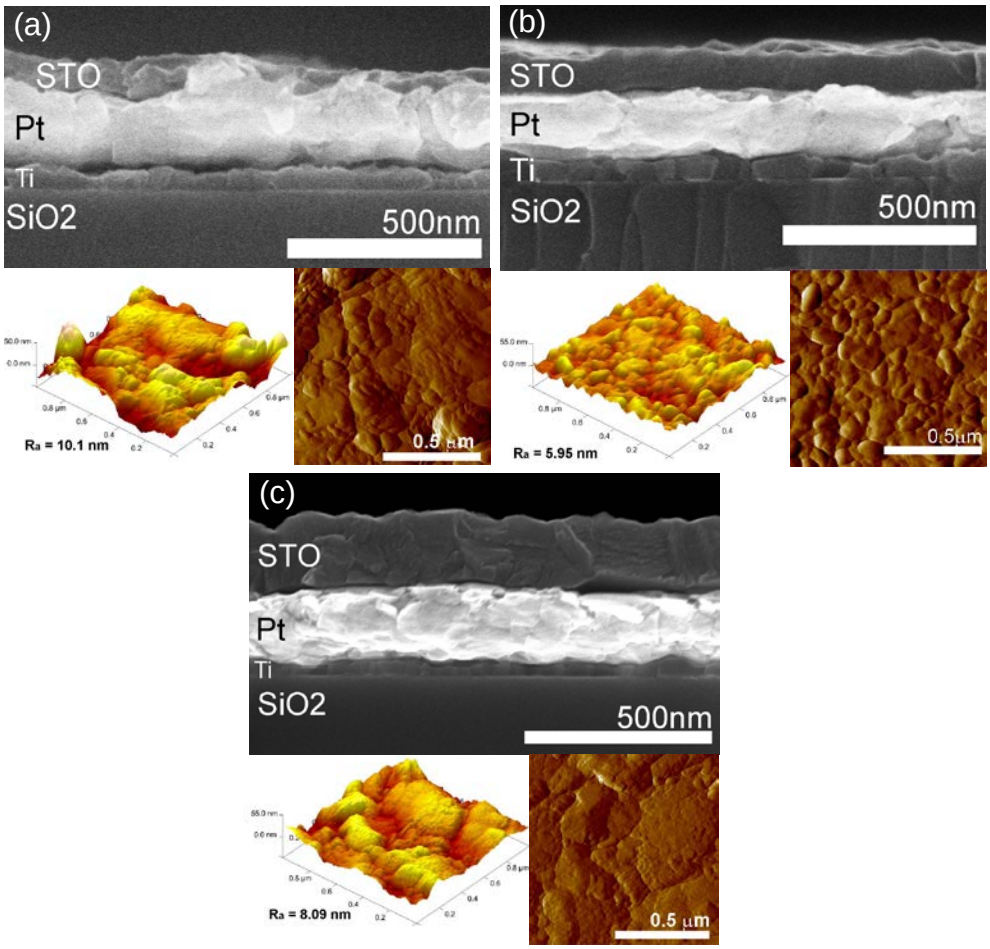

Fig. 5 SEM and AFM surface characterization data for a) 0.48-, b) 1.56-, and c) 2.91-nm/min growth rate samples. Average surface roughness (R_a) is also presented.

All 3 as-deposited samples showed dense, well-crystallized film microstructure as well as excellent delineation between STO film and the Pt BE. The selected samples were observed to contain a polycrystalline microstructure. It was observed that the STO thin films grown at the highest and lowest growth rates (0.48 and 2.91 nm/min, respectively) had much higher R_a values of 10.1 and 8.09 nm, respectively. The sample grown with a deposition rate of 1.56 nm/min under otherwise similar conditions yielded a well-developed surface with an

average surface roughness value of 5.95 nm. This sample was down-selected to perform dielectric property measurements to avoid dielectric losses associated with high surface roughness of the sample and, hence, losses due to a poor quality of a top electrode/sample surface contact.

5.4 Electrical Characterization

Preliminary dielectric response measurements (dielectric constant, loss tangent, and tunability) as a function of frequency and applied field were performed on STO thin film grown on PtSi substrate, which was deposited at 620 °C at a growth pressure of 15 Torr for 60 min at a total precursor mass flow rate of 60 μmole/min. The sample was annealed at 750 °C for 60 min in an O_2 gas environment, and circular Pt top electrodes of approximately 200-μ diameter and 100-nm thickness were then deposited on the STO film surface. The data are presented in Fig. 6.

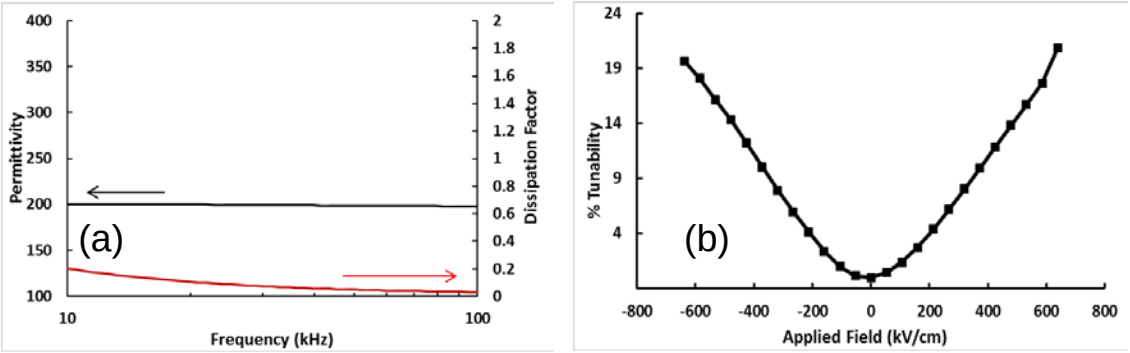

Fig. 6 a) Frequency dependence of dielectric loss and permittivity and b) tunability as a function of applied electric field

It is seen in Fig. 6 that no appreciable dispersion in the dielectric constant value was measured in the frequency range of 10–100 kHz. At 100 kHz, permittivity was 198 and dielectric loss was measured to be approximately 1%. Tunability increased almost symmetrically with negative and positive applied fields, and a maximum tunability of 20.85% was obtained with an applied field of 638.3 kV/cm.

6. Summary and Conclusions

Investigations were made in attempts to improve the compositional and structural quality of STO films as grown by the Gen 2 MOCVD system, as well as the homogeneity over the sample area. In all of the aforementioned aspects, sample quality was notably improved by modifications to both the hardware and growth parameters. Because of the many variables involved in the MOCVD process, spanning hardware, user software, and controllable growth parameters, there is still a notable element of irreproducibility in the STO films grown by the Gen 2 system. In the future, many more investigations must be conducted into the role of each of the controllable growth parameters as well as elements such as the precursor performance with respect to temperature, with the goal of optimization and stabilization across depositions. A study will be conducted to further investigate the variation and common elements of simultaneous film growth of STO on various single-crystal substrates such as MgO, Al_2O_3, and $LaAlO_3$.

7. References

1. Kong LB, Li S Zhang TS, Zhai JW, Boey FYC, Ma J. Electrically tunable dielectric materials and strategies to improve their performances. Progress in Materials Science. 2010;55:840–893.

2. Dey SP, Alluri V. PE-MOCVD of dielectric thin films: challenges and opportunities. MRS Bulletin. 1996;21:44–48.

3. Ohring, M. Materials science of thin films. 2nd edition. Waltham (MA): Academic Press; 2001.

4. Kern W, Schuegraf KK. Deposition technologies and applications: introduction and overview. In: Seshan K, editor. Handbook of thin film deposition processes and techniques. 2nd edition. Norwich (NY): William Andrew Publishing; 2001. p. 11–43.

5. Subramanyam G et al. Challenges and opportunities for multi-functional oxide thin films for voltage tunable radio frequency/microwave components. Journal of Applied Physics. 2013;114:191301.

6. Moeckly BH, Zhang YM. Strontium titanate thin films for tunable $YBa_2Cu_3O_7$ microwave filters. IEEE Transactions on Applied Superconductivity. 2001;11:450–453.

7. Moeckly BH, Peng LSJ, Fischer GM. Tunable HTS microwave filters using strontium titanate thin films. IEEE Transactions on Applied Superconductivity. 2003;13:712–715.

8. Yamaguchi H, Matsubara S, Miyasaka Y. Reactive coevaporation synthesis and characterization of $SrTiO_3$ thin-films. Japanese Journal of Applied Physics, Part 1 – Regular Papers Short Notes & Review Papers. 1991;30: 2197–2199.

9. Tomio T, Miki H, Tabata H, Kawai T, Kawai S. Control of electrical-conductivity in laser-deposited $SrTiO_3$ thin-films with NB doping. Journal of Applied Physics. 1994;76:5886–5890.

10. GrosseHolz KO, Cillessen JFM, Waser R. Electrical characterization of semiconducting La doped $SrTiO_3$ thin films prepared by pulsed laser deposition. Applied Surface Science. 1996;96(8):784–790.

11. Yu Z, Ang C, Guo RY, Bhalla AS, Cross LE. Dielectric loss modes of $SrTiO_3$ thin films deposited on different substrates. Applied Physics Letters. 2002;80:1034–1036.

12. Boikov YA, Olsson E, Claeson T. Effect of interfaces on the dielectric response of a $SrTiO_3$ layer between metallic oxide electrodes. Physical Review B. 2006;74:6.

13. Hyun S, Char K. Effects of strain on the dielectric properties of tunable dielectric $SrTiO_3$ thin films. Applied Physics Letters. 2001;79:254–256.

14. James AR, Xi XX. Effects of buffer layer thickness and strain on the dielectric properties of epitaxial $SrTiO_3$ thin films. Journal of Applied Physics. 2002;92:6149–6152.

15. Kim L, Kim J, Jung D, Lee J. Strain effect on dielectric property of $SrTiO_3$ lattice: first-principles study. Thin Solid Films. 2005;475:97–101.

16. Xi XX, Li HC, Si WD, Sirenko AA, Akimov IA, Fox JR, Clark AM, Hao JH. Oxide thin films for tunable microwave devices. Journal of Electroceramics. 2000;4:393–405.

17. Petrov PK, Carlsson EF, Larsson P, Friesel M, Ivanov ZG. Improved $SrTiO_3$ multilayers for microwave application: growth and properties. Journal of Applied Physics. 1998;84:3134–3140.

18. Lee MB, Koinuma H. Structural and dielectric properties of epitaxial $SrTiO_3$ films grown on Si(100) substrate with TiN buffer layer. Journal of Applied Physics. 1997;81:2358–2362.

19. Liu XZ, Tao BW, Li YR. Effect of oxygen vacancies on nonlinear dielectric properties of $SrTiO_3$ thin films. Journal of Materials Science. 2007;42:389–392.

20. Breckenfeld E, Wilson R, Karthik J, Damodaran AR, Cahill DG, Martin LW. Effect of growth induced (non)stoichiometry on the structure, dielectric response, and thermal conductivity of $SrTiO_3$ thin films. Chemistry of Materials. 2012;24:331–337.

21. Li HC, Si WD, West AD, Xi XX. Thickness dependence of dielectric loss in $SrTiO_3$ thin films. Applied Physics Letters. 1998;73:464–466.

22. Tachiki M, Noda M, Yamada K, Kobayashi T. $SrTiO_3$ films epitaxially grown by eclipse pulsed laser deposition and their electrical characterization. Journal of Applied Physics. 1998;83:5351–5357.

23. Iwabuchi M, Kinoshita IK, Kobayashi HT. Reduction of pinhole leakage current of $SrTiO_3$ films by ARF excimer-laser deposition with shadow mask (eclipse method). Japanese Journal of Applied Physics Part 2 – Letters. 1994;33:L610–L612.

24. Roy D, Peng CJ, Krupanidhi SB. Excimer laser ablated strontium-titanate thin-films for dynamic random-access memory applications. Applied Physics Letters. 1992;60:2478–2480.

25. Rao GM, Krupanidhi SB. Study of electrical-properties of pulsed excimer-laser deposited strontium-titanate films. Journal of Applied Physics. 1994;75:2604–2610.

26. Boikov TA, Claeson T. Dielectric response of epitaxial (100)$SrTiO_3$ films between electrodes of $SrRuO_3$ or high-T-C superconducting $YBa_2Cu_3O_7$-delta. Physica C. 2000;336:300–311.

27. Ohring, M. Plasma and ion beam processing of thin films. In: Ohring M, editor. Materials science of thin films. 2nd ed. San Diego (CA): Academic Press; 2002. p. 203–275.

28. Boesch DS, Son J, LeBeau JM, Cagnon J, Stemmer S. Thickness dependence of the dielectric properties of epitaxial $SrTiO_3$ films on (001)Pt/$SrTiO_3$. Applied Physics Express. 2008;1:3.

29. Son J, Cagnon J, Finstrom NH, Boesch DS, Lu JW, Stemmer S. Relationship between defects and the dielectric and transport properties of SrTiO(3) thin films. ISAF 2008. Proceedings of the 17th IEEE International Symposium on the Applications of Ferroelectrics; 2008 Feb 23–28; Santa Fe, NM. Piscataway (NJ): Institute of Electrical and Electronics Engineers; c2008. p. 82–83.

30. Son J, Stemmer S. Thermal leakage characteristics of Pt/$SrTiO_3$/Pt structures. Journal of Vacuum Science & Technology A. 2008;26:555–557.

31. Ryen L, Olsson E, Madsen LD, Wang X, Edvardsson CNL, Jacobsen SN, Helmersson U, Rudner S, Wernlund LD. Microstructure and microwave dielectric properties of epitaxial $SrTiO_3$ films on $LaAlO_3$ substrates. Journal of Applied Physics. 1998;83:4884–4890.

32. Abe K, Komatsu S. Measurement and thermodynamic analyses of the dielectric-constant of epitaxially grown $SrTiO_3$ films. Japanese Journal of Applied Physics Part 2 – Letters. 1993;32:L1157–L1159.

33. Gorrie CW, Sigdel AK, Berry JJ, Reese BJ, van Hest M, Holloway PH, Ginley DS, Perkins JD. Effect of deposition distance and temperature on electrical, optical and structural properties of radio-frequency magnetron-sputtered gallium-doped zinc oxide. Thin Solid Films. 2010;519:190–196.

34. Kumar C, Mansingh A. Effect of target-substrate distance on the growth and properties of RF-sputtered indium tin oxide-films. Journal of Applied Physics. 1989;65:1270–1280.

35. Komatsu S, Abe K, Fukushima N. Effects of ambient gas on dielectric constant of sputtered $SrTiO_3$ epitaxial thin films. Japanese Journal of Applied Physics Part 1 – Regular Papers Short Notes & Review Papers. 1998;37:5651–5654.

36. Park WY, Ahn KH, Hwang CS. Effects of in-plane compressive stress on electrical properties of $(Ba,Sr)TiO_3$ thin film capacitors prepared by on- and off-axis RF magnetron sputtering. Applied Physics Letters. 2003;83:4387–4389.

37. Zhu S, Su CH, Lehoczky SL, Peters P, George MA. Pressure effects in ZnO films using off-axis sputtering deposition. Journal of Crystal Growth. 2000; 211:106–110.

38. Abe K, Komatsu S. Dielectric-constant and leakage current of epitaxially grown and polycrystalline $SrTiO_3$ thin-films. Japanese Journal of Applied Physics Part 1 – Regular Papers Short Notes & Review Papers. 1993;32:4186–4189.

39. Itsumi MA, Ohfuji S, Akiya H. Electron-cyclotron-resonance sputtered $SrTiO_3$ thin films. Japanese Journal of Applied Physics. 1996;35:4963.

40. Pennebaker WB. RF sputtered strontium titanate films. IBM Journal of Research and Development. 1969;13(6):686–695.

41. Peng CJ, Hu H, Krupanidhi SB. Electrical properties of strontium-titanate thin-films by multi-ion-beam reactive sputtering technique. Applied Physics Letters. 1993;63:1038–1040.

42. Lu JW, Schmidt SY, Ok W, Keane SP, Stemmer S. Contributions to the dielectric losses of textured $SrTiO_3$ thin films with Pt electrodes. Journal of Applied Physics. 2005;98:9.

43. Ohring M. Epitaxy. In: Ohring M, editor. Materials science of thin films. 2nd Ed. San Diego (CA): Academic Press; 2002. p. 417–494.

44. Kim DW, Kim DH, Kang BS, Noh TW, Shin S, Khim ZG. Atomic control of homoepitaxial $SrTiO_3$ films using laser molecular beam epitaxy. Physica C. 1999;313:246–254.

45. Chang WT, Kirchoefer SW, Bellotti JA, Qadri SB, Pond JM, Haeni JH, Schlom DG. In-plane anisotropy in the microwave dielectric properties of $SrTiO_3$ films. Journal of Applied Physics. 2005;98:7.

46. Migita HS, Xiong SB, Fujino H, Kasai Y, Sakai S. Surface morphology and dielectric properties of stoichiometric and off-stoichiometric $SrTiO_3$ thin films grown by molecular beam epitaxy. Japanese Journal of Applied Physics Part 2 – Letters. 1999;38:L1535–L1537.

47. Bhuiyan MNK, Matsuda A, Yasumura T, Tambo T, Tatsuyama C. Study of epitaxial $SrTiO_3$ (STO) thin films grown on Si(001): 2 x 1 substrates by molecular beam epitaxy. Applied Surface Science. 2003;216:590–595.

48. Hao JH, Luo Z, Gao J. Effects of substrate on the dielectric and tunable properties of epitaxial $SrTiO_3$ thin films. Journal of Applied Physics. 2006; 100:5.

49. Chang W, Kirchoefer SW, Pond JM, Bellotti JA, Qadri SB, Haeni JH, Schlom DG. Room-temperature tunable microwave properties of strained $SrTiO_3$ films. Journal of Applied Physics. 2004;96:6629–6633.

50. Wu ZP, Huang W, Hao JH. Growth mode and dielectric properties in laser MBE grown multilayer of SrTiO(3) and YBa(2)Cu(3)O(y). Vacuum. 2010; 8:639–642.

51. Hao JH, Gao J, Wong HK. Laser molecular beam epitaxy growth and properties of $SrTiO_3$ thin films for microelectronic applications. Thin Solid Films. 2006;515:559–562.

52. Nakamura T, Tokuda H, Tanaka S, Iiyama M. Dielectric-properties of $SrTiO_3$ thin-films grown by ozone-assisted molecular-beam epitaxy. Japanese Journal of Applied Physics Part 1 – Regular Papers Short Notes & Review Papers. 1995;34:1906–1910.

53. Wu, ZP, Huang W, Wong, KH, Hao JH. Structural and dielectric properties of epitaxial SrTiO(3) films grown directly on GaAs substrates by laser molecular beam epitaxy. Journal of Applied Physics. 2008;104:3.

54. Jalan B, Moetakef P, Stemmer S. Molecular beam epitaxy of $SrTiO_3$ with a growth window. Applied Physics Letters. 2009;95:3.

55. Cole MW, Toonen RC, Hirsch SG, Ivill M, Ngo E. Hubbard C, Ramanathan S, Podpirka A. An elegant post-growth process science protocol to improve the material properties of complex oxide thin films for tunable device applications. Integrated Ferroelectrics. 2011;126:34–46.

56. Weiss CV, Zhang J, Spies M, Abdallah LS, Zollner S, Cole MW, Alpay SP. Bulk-like dielectric properties from metallo-organic solution-deposited $SrTiO_3$ films on Pt-coated Si substrates. Journal of Applied Physics. 2012;111:9.

57. Ma JH, Sun JL, Meng XJ, Lin T, Shi FW, Chu JH. Dielectric and interface characteristics of $SrTiO_3$ with a MIS structure. Acta Physica Sinica. 2005;54:1390–1395.

58. Kamalasanan, MN, Kumar ND, Chandra S. Structural, optical, and dielectric-properties of sol-gel derived $SrTiO_3$ thin-films. Journal of Applied Physics. 1993;74:679–686.

59. Thomas R, Dube DC, Kamalasanan MN, Chandra, S, Bhalla AS. Structural, electrical, and low-temperature dielectric properties of sol-gel derived $SrTiO_3$ thin films. Journal of Applied Physics. 1997; 82:4484–4488.

60. Tsuzuki A, Kato K, Kusumoto K, Torii Y. Sr/Ti ratio dependence of the dielectric properties of $SrTiO_3$ thin films prepared by sol-gel method. Journal of Materials Science Letters. 1997;16:1652–1653.

61. Leite ER, Sousa CMG, Longo E, Varela JA. Influence of polymerization on the synthesis of $SrTiO_3$ 1. characteristics of the polymeric precursors and their thermal-decomposition. Ceramics International. 1995;21:143–152.

62. Pontes FM, Lee EJH, Leite ER, Longo E, Varela JA. High dielectric constant of $SrTiO_3$ thin films prepared by chemical process. Journal of Materials Science. 2000;35:4783–4787.

63. Pontes FM, Leite ER, Lee EJH, Longo E, Varela JA. Preparation, microstructural and electrical characterization of $SrTiO_3$ thin films prepared by chemical route. Journal of the European Ceramic Society. 2001;21:419–426.

64. Gao YF, Masuda Y, Koumoto K. Dielectric characteristics of $SrTiO_3$ precursor thin film prepared on self-assembled monolayers by the liquid phase deposition method. Electroceramics in Japan VI. 2003;248:73–76.

65. Chou HY, Chen TM, Tseng TY. Dielectric and electrical properties of SrTiO(3+/-y)-(SiO2)(x) thin films. Journal of Physics D – Applied Physics. 2005;38:2446–2451.

66. Hofman W, Hoffmann S, Waser, R. Dopant influence on dielectric losses, leakage behaviour, and resistance degradation of $SrTiO_3$ thin films. Thin Solid Films. 1997;305:66–73.

67. Trepakov VA, Savinov ME, Okhay I, Tkach A, Vilarinho PM, Kholkin AL, Gregora I, Jastrabik L. Dielectric permittivity and Cr3+ impurity ion probe luminescence in $SrTiO_3$ sol-gel ceramics. Journal of the European Ceramic Society. 2007;27:3705–3707.

68. Hübert T, Beck U, Kleinke H. Amorphous and nanocrystalline $SrTiO_3$ thin films. Journal of Non-Crystalline Solids. 1996:196:150–154.

69. Jiang SW, Zhang QY, Li YR, Zhang Y, Sun XF, Jiang B. Structural characteristics of $SrTiO_3$ thin films processed by rapid thermal annealing. Journal of Crystal Growth. 2005;274:500–505.

70. Schwartz RW, Schneller T, Waser R. Chemical solution deposition of electronic oxide films. Comptes Rendus Chimie. 2004;7:433–461.

71. Dawley JT, Clem PG. Dielectric properties of random and < 100 > oriented $SrTiO_3$ and $(Ba,Sr)TiO_3$ thin films fabricated on < 100 > nickel tapes. Applied Physics Letters. 2002;81:3028–3030.

72. Toda M, Sasaki Y, Kurihashi Y, Umeda M, Fukagawa M, Tamura M, Kosugi Y, Kusuhar M. Thin film formations of ferroelectric material Bi(3)Nd(1)Ti(3)O(12) (BNT), high-K materials SrTiO(3) (STO) and Nb-doped SrTiO(3)(Nb-STO) by newly developed MOCVD system. Proceedings of the 16th IEEE International Symposium on the Applications of Ferroelectrics; 2007 May 27–30; Nara-City, Japan. Piscataway (NJ): IEEE; c2007. p. 142–145.

73. R. Hiskes, Dicarolis SA, Jacowitz RD, Lu Z, Feigelson RS, Route RK, Young JL. Single source MOCVD of epitaxial oxide thin-films. Journal of Crystal Growth. 1993;128:781–787.

74. Dhote AM, Meier AL, Towner DJ, Wessels BW, Ni J, Marks TJ. Low temperature deposition of epitaxial $BaTiO_3$ films in a rotating disk vertical MOCVD reactor. Journal of Vacuum Science & Technology B. 2005;23: 1674–1678.

75. Pierson HO. Metallo-organic CVD (MOCVD). In: Pierson HO, editor. Handbook of chemical vapor deposition (CVD). 2nd ed. Norwich (NY): William Andrew Publishing; 1999. p. 84–107.

76. Krumdieck SP. CVD reactors and delivery system technology. In: Chemical vapour deposition: precursors. London (UK): The Royal Society of Chemistry; 2009. p. 37–92.

77. Gadgil PN. Optimization of a stagnation point flow reactor design for metalorganic chemical-vapor-deposition by flow visualization. Journal of Crystal Growth. 1993;134:302–312.

78 Durst F, Kadinskii L, Peric M, Schafer M. Numerical study of transport phenomena in MOCVD reactors using a finite volume multigrid solver. Journal of Crystal Growth. 1992;125:612–626.

79. Jansen AN, Orazem ME, Fox BA, Jesser WA. Numerical study of the influence of reactor design on MOCVD with a comparison to experimental data. Journal of Crystal Growth 1991;112:316–336.

80 Hampdensmith MJ, Kodas TT. Chemical-vapor-deposition of metals 1. an overview of CVD processes. Chemical Vapor Deposition. 1995;1:8–23.

81. Tripathi AB. In-situ diagnostics for metalorganic chemical vapor deposition of YBCO. In: Engineering and applied science. Pasadena (CA): California Institute of Technology; 2001.

82. Funakubo H, Takeshima Y, Nagano D, Saiki A, Shinozaki K, Mizutani N. Deposition conditions of $SrTiO_3$ films on various substrates by CVD and their dielectric properties. Thin Solid Films. 1998;334:71–76.

83. Liang S, Chern CS, Shi ZQ, Lu P, Safari A, Lu Y, Kear BH, Hou SY. Epitaxial growth of $SrTiO_3/YBa_2Cu_3O_7{-}x$ heterostructures by plasma-enhanced metalorganic chemical vapor deposition. Applied Physics Letters. 1994;64:3563.

84. Yamaguchi H, Lesaicherre P-Y, Sakuma T, Miyasaka Y, Ishitani A, Yoshida M. Structural and electrical characterization of $SrTiO_3$ thin-films prepared by metal-organic chemical-vapor-deposition. Japanese Journal of Applied Physics Part 1 – Regular Papers Short Notes & Review Papers. 1993;32:4069–4073.

85. Cho HJ, Lee JM, Shin JC, Kim HJ. Electrical and microstructural properties of $SrTiO_3$ thin films deposited by metalorganic chemical vapor deposition. Integrated Ferroelectrics. 1997;14:115–122.

86. Grill A. Kane W, Beach D, Laibowitz R, Shaw T. Preparation of strontium-titanate films by MOCVD. Integrated Ferroelectrics. 1995;7:75–83.

87. Kang CS et al. Preparation and electrical properties of $SrTiO_3$ thin films deposited by liquid source metal-organic chemical vapor deposition (MOCVD). Japanese Journal of Applied Physics Part 1 – Regular Papers Short Notes & Review Papers. 1996;35:4890–4895.

88. Lee SW, Kwon OS, Han JH, Hwang CS. Enhanced electrical properties of SrTiO(3) thin films grown by atomic layer deposition at high temperature for dynamic random access memory applications. Applied Physics Letters. 2008;92:3.

89. Chung WY, Kim DH, Cho YS. Modelling of Cu thin film growth by MOCVD process in a vertical reactor. Journal of Crystal Growth. 1997;180: 91–97.

90. Ingle NK, Mountziaris TJ. The onset of transverse recirculations during flow of gases in horizontal ducts with differentially heated lower walls. Journal of Fluid Mechanics. 1994;277:249–269.

List of Symbols, Abbreviations, and Acronyms

AFM	atomic force microscopy
ALD	atomic layer deposition
Ar	argon
ARL	US Army Research Laboratory
Au	gold
BE	PtSi
CSD	chemical solution deposition
CVD	chemical vapor deposition
EDS	energy dispersive spectroscopy
LAO	lanthanum aluminate ($LaAlO_3$)
LSMO	lanthanum strontium manganite ($La_xSr_{1-x}MnO_3$)
MBE	molecular beam epitaxy
MgO	magnesium oxide
MOCVD	metalorganic chemical vapor deposition
MOSD	metalorganic solution deposition
O_2	oxygen
PEMOCVD	plasma-enhanced metalorganic chemical vapor deposition
PLD	pulsed laser deposition
Pt	platinum
PtSi	platinized silicon ($Pt/Ti/SiO_2/Si$)
R_a	average surface roughness
RF	radio frequency
sccm	standard cubic centimeters per minute
SEM	scanning electron microscopy
Si	silicon

Sr	strontium
SrO	strontium oxide
SRO	strontium ruthenate ($SrRuO_3$)
STO	strontium titanate ($SrTiO_3$)
Ti	titanium
TiO_2	titanium dioxide
UV	ultraviolet
XRD	X-ray diffraction
YBCO	yttrium barium copper oxide ($YBa_2Cu_3O_7$)

1 (PDF) DEFENSE TECHNICAL INFORMATION CTR DTIC OCA

2 (PDF) DIRECTOR US ARMY RESEARCH LAB RDRL CIO LL IMAL HRA MAIL & RECORDS MGMT

1 (PDF) GOVT PRINTG OFC A MALHOTRA

3 (PDF) DIR USARL RDRL WMM E S HIRSCH C HUBBARD E NGO

INTENTIONALLY LEFT BLANK.